Lattice Thermal Conductivity of Embedded Nanoparticle Composites: The Role of Particle Size Distribution

Theodore Maranets^{1,*}, Haoran Cui¹, and Yan Wang¹

¹Department of Mechanical Engineering, University of Nevada, Reno, Reno, NV, 89557, USA

*Corresponding author. E-mail address: tmaranets@nevada.unr.edu (T. Maranets)

Abstract

Nanoparticles embedded within a crystalline solid serve as impurity phonon scattering centers that reduce lattice thermal conductivity, a desirable result for thermoelectric applications. Most studies of thermal transport in nanoparticle-laden composite materials have assumed the nanoparticles to possess a single size. If there is a distribution of nanoparticle sizes, how is thermal conductivity affected? Moreover, is there a best nanoparticle size distribution to minimize thermal conductivity? In this work, we study the thermal conductivity of nanoparticle-laden composites through a molecular dynamics approach which naturally captures phonon scattering processes more rigorously than previously used analytical theories. From thermal transport simulations of a systematic variety of nanoparticle configurations, we empirically formulate how nanoparticle size distribution, particle number density, and volume fraction affect the lattice thermal conductivity. We find at volume fractions below 10%, the particle number density is by far the most impactful factor on thermal conductivity and at fractions above 10%, the effect of the size distribution and number density is minimal compared to the volume fraction. In fact, upon comparisons of configurations with the same particle number density and volume fractions, the lattice thermal conductivity of a single nanoparticle size can be lower than that of a size distribution which contradicts intuitions that a single size would attenuate phonon transport less than a spectrum of sizes. The random alloy, which can be considered as a single size configuration of maximum particle number density where the nanoparticle size is equal to the lattice constant, is the most performant in thermal conductivity reduction at volume fractions below 10%. We conclude that nanoparticle size distribution only plays a minor role in affecting lattice thermal conductivity with the particle number density and volume fraction being the more significant factors that should be considered in fabrication of nanoparticle-laden composites for potential improved thermoelectric performance.

1 Introduction

Magnification of phonon scattering to reduce lattice thermal conductivity has been a critical focus in nano-scale-engineering efforts to improve the performance of thermoelectric materials [1]. The thermoelectric figure-of-merit of a material is proportional to the electrical conductivity divided by the thermal conductivity which can be considered as the sum of the electron and phonon contributions to thermal transport. To increase figure-of-merit, it is desired to increase electrical conductivity or reduce thermal conductivity, however, the electrical conductivity is directly proportional to the electron contribution to thermal conductivity per the Wiedemann-Franz law [2]. Therefore, modification of the electron transport will impact both electrical and thermal properties. To bypass this problem in the effort to improve the figure-of-merit, researchers have focused on lowering the phonon contribution to thermal transport, or the lattice thermal conductivity, by exploiting the differences in transport properties between electrons and phonons [3]. Particularly, lattice thermal conductivity reduces with increased phonon scattering, therefore, the thermoelectric material may be nano-structured to magnify phonon scattering opportunities with minimal modification to electron scattering [4].

Embedded nanoparticles, nano-scale sized dopant particulates embedded within a host lattice, can serve as impurity phonon scattering centers that reduce lattice thermal conductivity. Nanoparticle-laden composites have demonstrated promise as low cost, but high efficiency thermoelectric materials

[5]. Thus, it is of significant interest to study phonon transport behaviors through these composites to guide design of more performant thermoelectric materials. Several theoretical analyses of phonon scattering by mass-mismatched nanoparticles have been made to predict the thermal conductivity of nanoparticle-laden composites, however, most studies solely considered the nanoparticles to possess a single size [6] [7]. Minimal detail has been paid to the case where the nanoparticles possess a distribution of sizes. A nanoparticle size distribution may be influential in modifying thermal properties as materials possess a broad spectrum of phonons with varying contribution to lattice thermal conductivity [4].

Zhang and Minnich notably investigated the impact of a nanoparticle size distribution through an application of a Monte-Carlo optimization algorithm that identified a size distribution which best minimized a numerical thermal conductivity calculation of a Si/Ge composite considering phononnanoparticle scattering [8]. While conceptually illustrative of the effect of nanoparticle size distribution on lattice thermal conductivity, the implemented analytical expression of the phonon-nanoparticle scattering rate was non-mode-resolved and poorly describes wavelength dependence through an approximate "patching" solution of the short and long wavelength regimes, derived from an analytical treatment of phonons as electromagnetic waves [9]. We argue that this simplified analysis provides little confidence to describing the true effect of a nanoparticle size distribution on lattice thermal transport.

Alternative methodologies, both analytical and computational, exist and have been used to investigate and model phonon-nanoparticle scattering [10] [11] [12] [7] [13]. Among the various tools employed, molecular dynamics (MD) emerges as a rigorous approach where phonon transport as the discrete modes of lattice vibrations can be explicitly modeled [14]. In this work, we apply MD simulation techniques to study the lattice thermal conductivity of nanoparticle-laden composites. We particularly examine how various nanoparticle size distributions, both irrationally and rationally designed, influence the lattice thermal transport. Furthermore, we also investigate the roles of particle number density and volume fraction to formulate a holistic empirical model of lattice thermal conductivity modification in the particulate solid medium.

2 Methodology

We perform nonequilibrium molecular dynamics (NEMD) simulations to predict the lattice thermal conductivity of a systematic variety of embedded nanoparticle composites. We chose a Lennard-Jonnes (LJ) FCC structure as our model material system for reduced computational cost. The LJ model for interactions is given as [15]

$$\phi_{ij}(r_{ij}) = 4\epsilon \left[\left(\frac{\sigma}{r_{ij}} \right)^{12} - \left(\frac{\sigma}{r_{ij}} \right)^{6} \right]$$
 (1)

where r_{ij} is the interatomic distance between atoms i and j and ϵ and σ are parameters. The host matrix has a molecular weight of $40 \, g/mol$, approximately the weight of solid argon, while the nanoparticle matrix has a molecular weight of $90 \ q/mol$. The atomic mass of the nanoparticle has been chosen to be 2.25 times that of the matrix material for two reasons. First, it falls within the range of atomic mass ratios of the material pairs used in previous experimental studies of phonon transport properties in heterogeneous structures or nanocomposite materials. Examples include Si/Ge (2.59), Bi₂Te₃/Sb₂Te₃ (1.28 when averaged as a single material or 1.72 for Sb/Bi), and GaAs/AlAs (1.42 when averaged as a single material or 2.58 for Ga/Al) [16] [17]. Second, we have followed the same choice of atomic mass ratio as in our previous studies on superlattices, because we anticipate comparing nanocomposite systems with superlattice structures in the future [18] [19]. The parameter set of $\epsilon_{Ar} = 0.0104 \ eV$, $\sigma_{Ar} = 0.34$ nm, and a cutoff radius of $2.5\sigma_{Ar}$ has been used in previous studies on LJ-modeled solid argon [20] [21]. In this work, we use $\epsilon = 16\epsilon_{Ar}$ for the interactions of all atom types to mimic stronger bonded materials such as Si/Ge and GaAs/AlAs as done in previous LJ NEMD investigations [22] [23]. We forgo inclusion of an elastic contrast as it is an added degree of complexity to the scattering system and impurity scattering is shown to be primarily due to the mass contrast [24]. The relaxed lattice constant determined from MD relaxation commands for the given material model was a = 5.2686 Å.

Discussion of the specifics of lattice thermal conductivity prediction from the NEMD method can be found in other works [14] [26] [27]. A diagram of our simulation domain is presented in Figure 1. The dimensions of our hot and cold baths are 40 unit cells (UC) in the x direction and 29 UC in both y

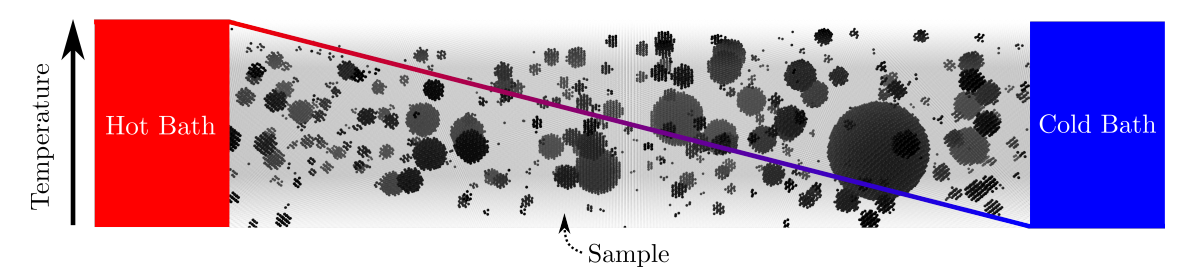


Figure 1: Nonequilibrium molecular dynamics (NEMD) system diagram. The fixed temperature difference between the hot and cold baths induces a heat flux through the sample from which the effective thermal conductivity κ can be calculated using Fourier's law at steady state. Sample image visualized using OVITO [25]

and z directions. The dimensions of the embedded nanoparticle composite "sample" located between the baths are 500 UC in the x direction (aligned along the [100] crystal orientation) and 29 UC in both y and z directions. The large cross-section is necessary to accommodate both large particles up to 10 nm diameter and a multiple number of particles in the cross-section. At 500 UC, the sample length is larger than the majority of phonon mean free paths contributing strongly to heat conduction in the pure host material, therefore, finite size effects typically associated with the NEMD method are minimal. From this, we forgo conducting simulations of different sized systems in order to extrapolate a bulk thermal conductivity value. The apparent thermal conductivity measurements from the NEMD simulations conducted in this work are reasonable estimates of the bulk thermal conductivity value. Periodic boundary conditions are applied to all three directions. We use a simulation time step of 1 fs according to the criterion in Reference [21]. Our specific NEMD simulations are conducted with the LAMMPS software package [28] in the following process. (1) Each atom is given a random initial velocity corresponding to a temperature of 5 K. (2) The entire system is relaxed in the isothermalisobaric (NPT) ensemble at zero pressure, and the temperature is increased from 5 K to 40 K in 1000 ps. (3) The entire system is relaxed in the NPT ensemble at zero pressure and 40 K. (4) A 7 Å layer of atoms at both ends of the simulation are frozen and kept such that fixed boundary conditions are applied in the x direction. (5) The simulation configuration is switched from the NPT ensemble to the microcanonical ensemble (NVE) and the hot and cold baths are maintained at temperatures of 60 K and 20 K, respectively using a Langevin thermostat. Step (5) lasts for 12000 ps to ensure the heat current through the system reaches steady state. Finally, the apparent thermal conductivity κ of the sample is evaluated using Fourier's law. Thermal conductivity prediction from the NEMD method is not significantly influenced by changes in the initialization of atom velocities as the system is forced into nonequilibrium by an applied temperature gradient [26]. Therefore, it is unnecessary to run multiple simulations with perturbations in initialization for statistical averaging. Consequentially, we conduct only one NEMD simulation for each sample configuration explored in this work.

3 Results and Discussion

3.1 Single Size Distribution and Random Alloy

3.1.1 Introduction

We first compute the thermal conductivity κ values for the both the composite with a single nanoparticle size and the random alloy to establish a quasi-control group for later comparison to composites possessing a distribution of nanoparticle sizes. The single size distribution for a fixed volume fraction f_v is constructed by first selecting a specific nanoparticle diameter D and then determining the number of such sized nanoparticles N that would satisfy the value of f_v . Then, the composite structure is generated by positioning N such spherical nanoparticles lattice-matched into the host matrix. For all composite configurations presented in this article, the nanoparticles are positioned randomly throughout the sample while ensuring no overlap. Since the total volume of the sample V in the NEMD simulation is the same in all configurations studied, the particle number density $N_T = N/V$ changes linearly with N and so in this article, we will equate direct changes in number of nanoparticles N to

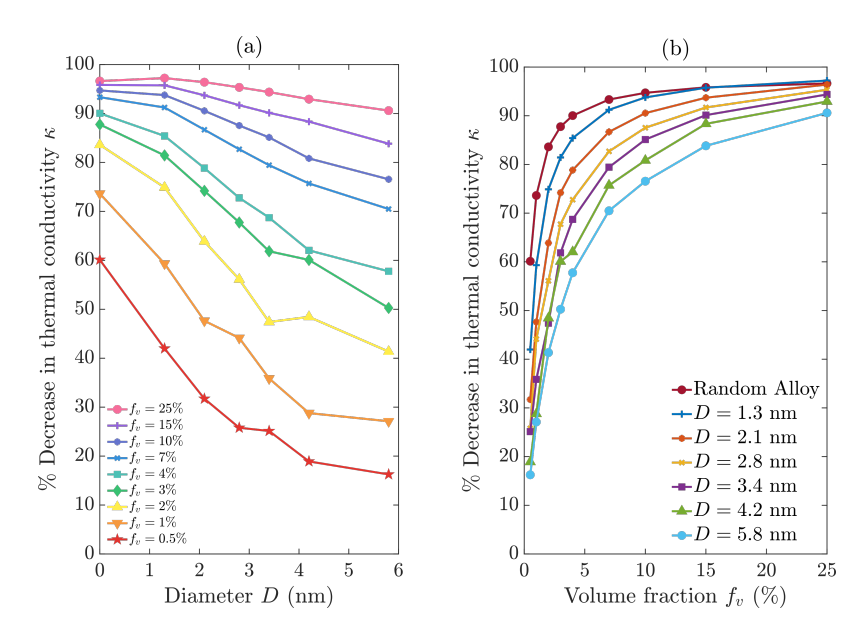


Figure 2: (a) Single size distribution percent decrease in thermal conductivity κ as a function of nanoparticle diameter D at different volume fractions f_v . (b) Single size distribution percent decrease in κ as a function of f_v for various values of D.

direct changes in particle number density N_T . In this sense, comparisons of single size distributions with the same f_v but differing D are effectively comparisons of different values of N. Furthermore, the random alloy which is the random substitution of host matrix atoms with impurity atoms, can be considered as a single size distribution of maximum possible N where the nanoparticle size is equal to the lattice constant.

3.1.2 Results and Discussion

We present the percent decrease in thermal conductivity κ for varying values of D at different volume fractions f_v in Figures 2a and 2b. Figure 2a reveals that for all values of f_v , the attenuation of lattice thermal transport increases as D decreases. This trend effectively means that for a fixed volume fraction, lattice thermal conductivity of the single size distribution decreases with increasing number of nanoparticles N. The slope of the trend is magnified at low values of f_v and gradually decreases as f_v increases. Most notably, at large volume fractions $f_v > 10\%$, there is minimal difference in κ as N is varied as seen in Figure 2b.

The data presented in Figures 2a and 2b suggest that for the single size distribution, at low values of f_v , κ is strongly dependent on N with higher N resulting in lower values of κ . This result agrees well with experimental data of thermal conductivity of (Bi,Sb)₂Te₃ ladened with SiC nanoparticles at fixed $f_v = 0.4\%$ where for a single size distribution, smaller nanoparticles were found to reduce thermal conductivity more effectively than larger sizes [29]. A direct comparison of thermal conductivity reduction is unavailable as the sizes of the experiment nanoparticles are too computationally expensive for MD simulation. As volume fraction is increased, we find κ does not vary as considerably with N, likely due to the volume of dopant material being large enough that the variation in sizes only has a minimal impact on κ . We also note for all volume fractions f_v tested below 10%, the random alloy configuration achieved the lowest thermal conductivity κ . At large $f_v > 10\%$, a few low D single size distribution possessed lower κ values than the random alloy, however, the difference was practically within the error of the NEMD thermal conductivity prediction. Additionally, it will be shown in later sections exploring other configurations, that the nanoparticle size distribution has minimal influence at large f_v . Finally, the reduction in κ with increasing f_v is consistent with previous experimental data on nanoparticle dispersion in the crystal matrix [30] [31] [32]. It should be mentioned that there must exist an optimal volume fraction of nanoparticles to achieve the lowest thermal conductivity for a specific particle size or size distribution. Analogous to binary alloys, the thermal conductivity of nanoparticle-laden composites initially decreases as the volume fraction of nanoparticles increases, but

it subsequently rises when the volume fraction of nanoparticles becomes sufficiently large, typically around 50%, resembling the characteristics of a pure nanoparticle material [8]. Given the anticipated nature of this phenomenon and the fact that our research is solely focused on investigating the influence of particle size and size distribution on thermal conductivity, we have made a deliberate decision to not explore volume fractions exceeding 25%.

3.2 Irrational Distributions

3.2.1 Introduction

In this section, we investigate the lattice thermal transport in composites possessing a distribution of nanoparticle sizes. We distinguish the different distributions as irrational and rational. The irrational distributions are composites with nanoparticle size distributions generated from common distribution functions used in the field of probability and statistics. The rational distribution is a size distribution generated from the lattice thermal conductivity spectrum of the host matrix in order to target the wavelengths that contribute most strongly to thermal transport. In this section, for the irrational distributions, we examine the thermal conductivity κ values of composites generated from the Gamma, Exponential, and Uniform distribution functions. To our knowledge at the time of writing, there is no experimental data on these distributions. Still, simulation agreement with experiment in the previous section gives us confidence in our methodology and thus following predictions and analyses.

3.2.2 Results and Discussion

Gamma Distribution We first present the results for the Gamma distribution at low, intermediate, and high volume fractions ($f_v = 1\%$, 4%, and 10%, respectively). The nanoparticle size distribution is constructed in the following process. (1) Values of f_v and N are selected and fixed. (2) A value of the shape parameter α is chosen and N random numbers, s, are generated from the corresponding probability density function p(s) of the one-parameter Gamma distribution

$$p(s) = \operatorname{Gamma}(\alpha, 1/\alpha) = \frac{1}{\Gamma(\alpha)} \alpha^{\alpha} s^{\alpha - 1} e^{-\alpha s}$$
 (2)

where Γ is the gamma function. (3) Those N numbers are normalized such that the mean $\langle s \rangle$ is unity and then a mean radius $\langle R \rangle$ is determined from the following equation

$$\langle R \rangle^3 = \frac{f_v V}{\sum \frac{4}{3} \pi s^3} \tag{3}$$

where V is the sample volume. (4) The nanoparticle radii in the composite are then set to $R = s\langle R \rangle$. Histograms of the mean-normalized nanoparticle diameters D = 2R at various shape parameter α values are shown in Figure 3.

First, we examine the configuration where N is set to the mean value of N for single size distributions ranging from D=1 nm to D=10 nm. For the remainder of this article, we will term this value of N as the "unfixed case". The percent decrease in thermal conductivity κ for varying values of α at different volume fractions f_v for the unfixed case are presented in Figure 4. For all volume fractions f_v , thermal conductivity κ is observed to decrease as shape parameter α is increased which corresponds to a narrowing of the distribution to a single nanoparticle size as seen in Figure 3. Due to the N value of the unfixed case being less than that of the single size distribution with D=1.3 nm, the nanoparticle size that the Gamma Unfixed distribution converges to is larger than 1.3 nm. For all α and f_v values tested, the Gamma Unfixed distribution did not possess a thermal conductivity lower than the reported single size distribution with larger N and the random alloy. This result means the Gamma distribution in the unfixed case is insufficient in improvement of thermal conductivity reduction over the single size distribution with larger N.

To provide further depth to this discussion, we repeated the investigation of κ variation with α in the case that N for the Gamma distribution exactly matched the value of N for the single size distribution with D=1.3 nm. We will term this configuration as the "fixed case" as we are fixing the value of N in a way to solely assess the difference in thermal conductivity between the distribution possessing a specific spectrum of nanoparticle sizes and the equivalent single size distribution. The results for the Gamma Fixed configuration are presented in Figure 5. Similar to the unfixed case,

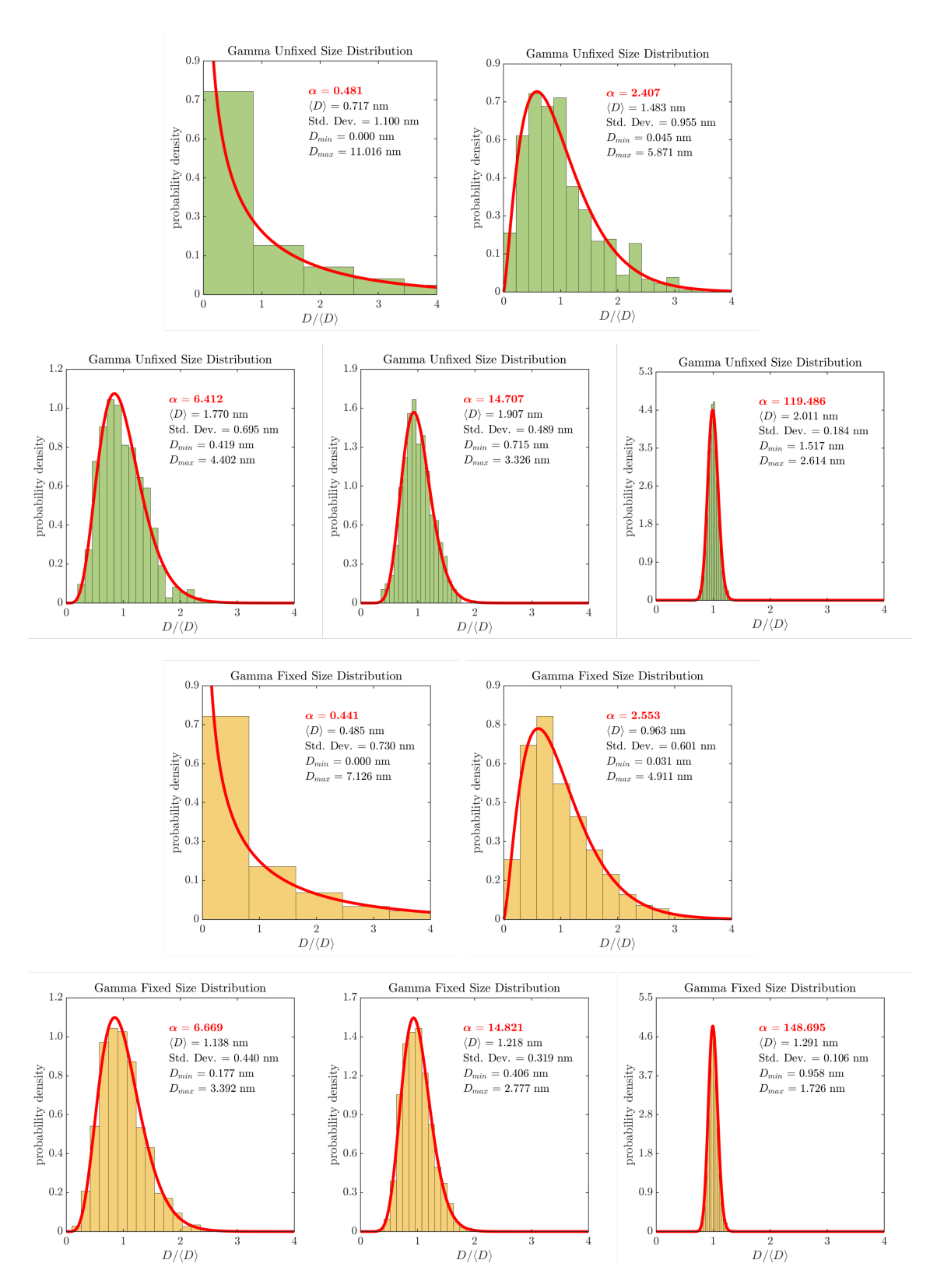


Figure 3: Normalized size distribution plots of the Gamma Unfixed and Gamma Fixed nanoparticle size distributions at $f_v = 4\%$. As shape parameter α increases, the distributions converges to a single size distribution. Changes in number of nanoparticles N between the unfixed to fixed cases leads to changes in the mean particle size, standard deviation, and the minimum and maximum sizes.

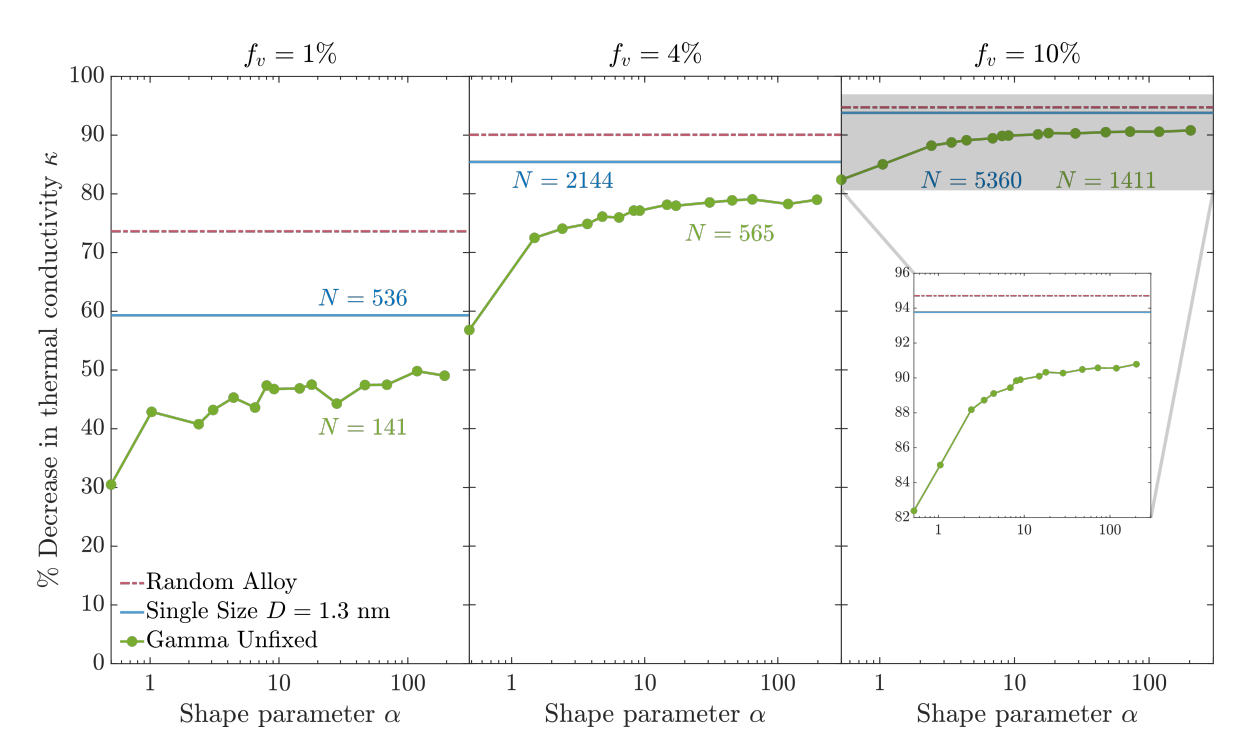


Figure 4: Gamma Unfixed distribution percent decrease in thermal conductivity κ for varying values of shape parameter α at different volume fractions f_v . For all α and f_v tested, the Gamma Unfixed distribution is unable to achieve a lower thermal conductivity than the single size distribution with D=1.3 nm and the random alloy. The result is likely due to a reduced particle number density rather than the specific spectrum of sizes.

the Gamma Fixed composite thermal conductivity κ decreases with increasing shape parameter α . The fixed case κ expectedly approaches the value of the single size as the distribution is narrowed. Most importantly, the data presented in Figure 5 reveals that like the unfixed case, the Gamma Fixed distribution is unable to achieve a thermal conductivity lower than the single size distribution and the random alloy up to high α for all f_v tested. Specifically, the low α values suggest that the attenuation of lattice thermal transport by the Gamma distribution can be less than the single size distribution with equivalent N. This result is a first example in this study of a nanoparticle size distribution possessing a spectrum of sizes being less performant in thermal conductivity reduction than a configuration with a single nanoparticle size when volume fraction and particle number density are identical between the two distributions. A possible explanation is that at low α , there is a significant amount of nanoparticles with diameters smaller than 1.3 nm which likely scatter phonons less strongly. The presence of a few nanoparticles with sizes larger than 1.3 nm is not sufficient to counteract the reduced phonon scattering by the greater number of smaller nanoparticles.

Additionally, we find in both the fixed and unfixed cases, the difference in thermal conductivity κ reduction between the Gamma distribution and the single size distribution decreases as volume fraction f_v increased. This result supports our conclusion made in the previous section that at large f_v , κ is minimally affected by variation in nanoparticles sizes and particle number density due to the presence of a large amount of dopant material in the host matrix.

Exponential Distribution The second irrational distribution we investigate is the Exponential distribution. The nanoparticle size distribution is constructed in the following process. (1) Values of f_v and N are selected and fixed. (2) A value of the rate parameter μ is chosen and N random numbers, s, are generated from the corresponding probability density function p(s) of the Exponential distribution

$$p(s) = \exp\left(\mu\right) = \mu e^{-\mu s} \tag{4}$$

(3) Considering s to be a set of diameters in nm, the distribution is rescaled to be a set of radii in \mathring{A} and then a mean radius $\langle R \rangle$ is determined from Equation 3. (4) The nanoparticle radii in the composite are

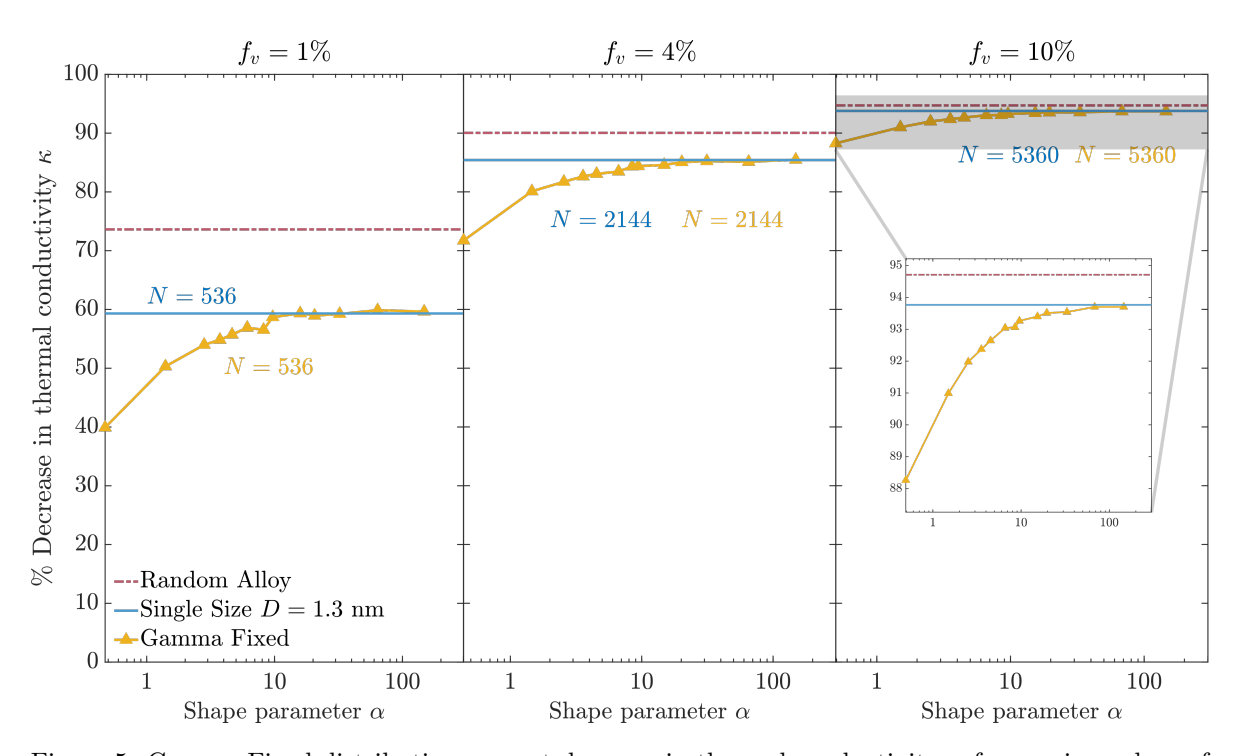


Figure 5: Gamma Fixed distribution percent decrease in thermal conductivity κ for varying values of shape parameter α at different volume fractions f_v . The fixed case κ expectedly approaches the value of the single size as the distribution is narrowed, however at low α , the Gamma Fixed distribution is unable to achieve a thermal conductivity lower than the single size distribution and the random alloy. This result is likely due to there being a significant amount of nanoparticles with diameters smaller than 1.3 nm which likely scatter phonons less strongly. The presence of a few nanoparticles with sizes larger than 1.3 nm is not sufficient to counteract the reduced phonon scattering by the greater number of smaller nanoparticles.

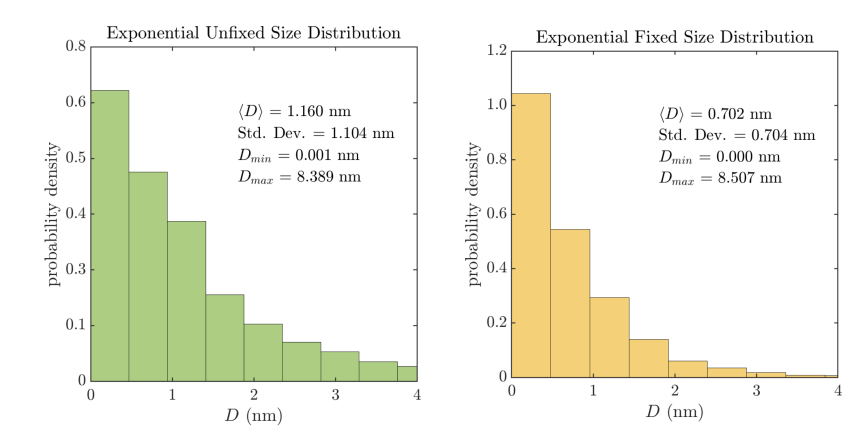


Figure 6: Size distribution plots of the Exponential Unfixed and Exponential Fixed nanoparticle size distributions at $f_v = 4\%$. Changes in N between the unfixed and fixed cases corresponds to changes in mean diameter and standard deviation.

then set to $R = s\langle R \rangle$. Due to the properties of the Exponential distribution and our specific fixing of volume fraction f_v and number of nanoparticles N, there is effectively only one possible configuration of an Exponential nanoparticle size distribution for specified values of f_v and N. Thus, we examine the thermal conductivity of a composite with this configuration at different values of f_v for the fixed and unfixed cases of N. Histograms of the nanoparticle diameters D for the fixed and unfixed cases are shown in Figure 6.

The results of the percent decrease in thermal conductivity κ for the Exponential distribution and its comparison to the single size distribution with D=1.3 nm and the random alloy are presented in Figure 7. For all tested volume fractions f_v and both the fixed and unfixed cases of N, the thermal conductivity κ reduction of the Exponential distribution is less than both the single size distribution and the random alloy as it was for the Gamma distribution. The fixed case result is a second example of a nanoparticle size distribution possessing a spectrum of sizes being less performant in thermal conductivity reduction than an equivalent single size distribution. This result is expected as the shape of the Exponential distribution, seen in Figure 6, is similar to the shape of the Gamma distribution, seen in Figure 3, at low shape parameter α . Furthermore, we see a repeat of the κ behavior at large f_v observed for prior distributions. The difference in thermal conductivity κ reduction between the Exponential distribution and the single size distribution decreases with increasing volume fraction f_v . This result is additional evidence supporting the conclusion that at large f_v , variation in nanoparticles sizes and particle number density has a minimal influence on κ ; the volume fraction being the dominant factor on lattice thermal transport.

Uniform Distribution The third and final irrational distribution we investigate is the Uniform distribution. The nanoparticle size distribution is constructed in the following process. (1) Values of f_v and N are selected and fixed. (2) A uniform distribution of N diameters s that ranges from 0 to some value D that satisfies f_v is determined via a brute force search. (3) The nanoparticle diameters are set to the found distribution. Histograms of the nanoparticle diameters D for the fixed and unfixed cases are shown in Figure 8.

The results of the percent decrease in thermal conductivity κ for the Uniform distribution and its comparison to the single size distribution with D=1.3 nm and the random alloy are presented in Figure 9. Similar to both the Gamma and Exponential distributions, for both fixed and unfixed cases, the Uniform distribution does not achieve a lower thermal conductivity κ than both the single size distribution and the random alloy. Additionally, the difference in κ between the Uniform distribution and the single size distribution decreases with increasing volume fraction f_v , just like the Exponential and Gamma configurations. However, upon comparison, the data in Figure 9 show that for all f_v , the thermal conductivity κ of the Uniform distribution is lower than the equivalent Exponential distribution and Gamma distribution up to high values of shape parameter α suggesting the Uniform distribution is more performant in thermal conductivity reduction than the other irrational distributions explored in this work.

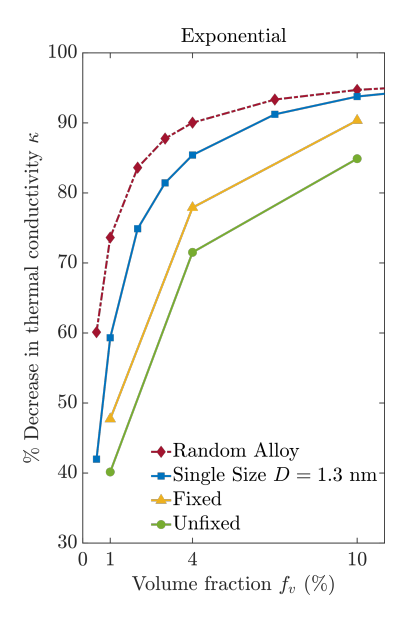


Figure 7: Exponential distribution percent decrease in thermal conductivity κ for various volume fractions f_v . In both the fixed and unfixed cases, the Exponential distribution is not able to achieve a thermal conductivity lower than the single size distribution with D=1.3 nm and the random alloy. This result is likely due to the shape of the distribution, seen in Figure 6, which features a large presence of small nanoparticles that scatter phonons less strongly.

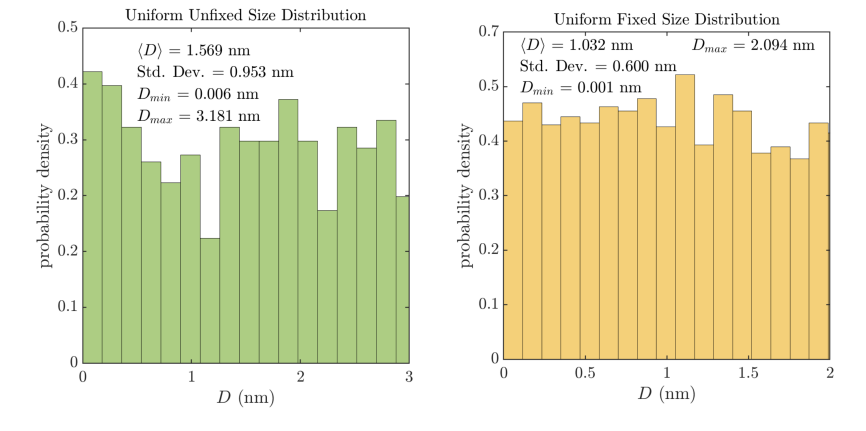


Figure 8: Size distribution plots of the Uniform Unfixed and Uniform Fixed nanoparticle size distributions at $f_v = 4\%$. The reduced uniformity in the unfixed distribution is due to a lower number of nanoparticles N. Changes in N correspond to changes in mean diameter and maximum particle size.

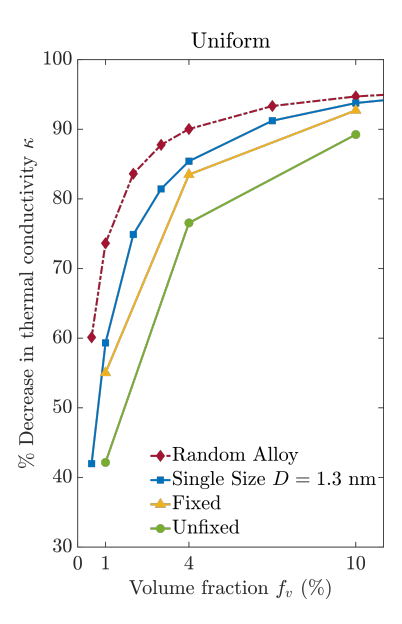


Figure 9: Uniform distribution percent decrease in thermal conductivity κ for various volume fractions f_v . In both the fixed and unfixed cases, the Uniform distribution is not able to achieve a thermal conductivity lower than the single size distribution with D=1.3 nm and the random alloy. The Uniform distribution is however, more performant in thermal conductivity reduction than the Exponential distribution and the Gamma distribution at low shape parameter α . This result exemplifies that size distribution contribution to κ is still non-negligible.

The key conclusion we identify from the tested irrational distributions is that for a fixed volume fraction and particle number density, an irrational size distribution is never able to outperform the single size distribution and is in most cases, less performant than the single size distribution. Furthermore, we found the results for the irrational distribution matched the inferences from the single size distribution data in the previous section. Specifically, (1) at low volume fractions, the particle number density is a more significant contributor to thermal conductivity reduction than the nanoparticle size distribution. (2) At large volume fractions, there are minimal differences in thermal conductivity reduction for changes in size distribution and particle number density. From these findings, we begin to formulate an understanding that size distribution is not the most influential factor in lattice thermal transport through a nanoparticle-laden composite. In fact, the particle number density and volume fraction are shown to be far more significant in modifying the lattice thermal conductivity than the specific nanoparticle sizes.

3.3 Rational Distribution

3.3.1 Introduction

In this section, we compute the percent decrease in thermal conductivity κ of a composite possessing a nanoparticle size distribution that approximately matches the thermal conductivity spectrum of the host matrix. Specifically, we computed the wavelength-dependent thermal conductivity and treated that function as a probability density function to which we construct the nanoparticle size distribution from, equating phonon wavelengths to nanoparticle radii. We term this configuration as the "rational distribution" as we are specifically targeting the wavelengths that contribute most to κ . Since we fix volume fraction f_v and the specific nanoparticle sizes, the number of nanoparticles N is not able to be user-defined and thus set to the value to which the rational distribution can satisfy the specified volume fraction f_v . In all configurations, N for the rational distribution was less than the N for the unfixed and fixed cases.

The thermal conductivity spectrum of the host matrix is determined from phonon normal mode analysis in equilibrium molecular dynamics simulations as molecular dynamics can model temperaturedependent anharmonic phonon scattering to higher orders than anharmonic lattice dynamics techniques [33] [14]. First, the normal mode coordinates $q_{\mathbf{k},\nu}(t)$ and spectral energy density $\Phi_{\mathbf{k},\nu}(\omega)$ are evaluated:

$$q_{\mathbf{k},\nu}(t) = \sum_{\alpha}^{3} \sum_{b}^{n} \sum_{l}^{N_{c}} \sqrt{\frac{m_{b}}{N_{c}}} u_{\alpha}^{l,b}(t) e_{b,\alpha}^{\mathbf{k},\nu*} \exp\left(i\mathbf{k} \cdot \boldsymbol{r_{0}^{l}}\right)$$
(5)

$$\Phi_{\mathbf{k},\nu}(\omega) = |\mathcal{F}[\dot{q}_{\mathbf{k},\nu}(t)]|^2 = \frac{C_{\mathbf{k},\nu}}{(\omega - \omega_{\mathbf{k},\nu}^A)^2 + (\tau_{\mathbf{k},\nu}^{-1})^2/4}$$
(6)

where $u_{\alpha}^{l,b}(t)$ represents the α th component of the displacement of the bth basis atom in the lth unit cell, N_c is the total number of primitive unit cells in the entire system, m_b is the mass of the bth basis atom, t is time, e is the phonon eigenvector, \mathbf{k} is the phonon wavevector, ν is the phonon mode, and r_0^l is the equilibrium position of the lth unit cell. In Equation 6, the Fourier transform \mathcal{F} of the time derivative of the normal mode coordinate is fitted to a Lorentzian function to obtain the peak frequency position $\omega_{\mathbf{k},\nu}^A$ and spectral phonon scattering rate $\tau_{\mathbf{k},\nu}^{-1}$ which is the inverse of the phonon relaxation time $\tau_{\mathbf{k},\nu}$. $C_{\mathbf{k},\nu}$ is a mode-specific constant. The phonon dispersion curves are obtained by connecting the peak frequency position with continuous and differentiable curves from which phonon group velocity $v_g = \frac{\partial \omega}{\partial k}$ can be calculated using central difference technique. The [100] thermal conductivity spectrum is then calculated from kinetic theory:

$$\kappa(\mathbf{k}) = \sum_{\nu} c_{ph} v_g^2 \tau_{\mathbf{k},\nu} \tag{7}$$

where c_{ph} is the phonon specific heat. As molecular dynamics is a classical system, the specific heat may be evaluated as $c_{ph} = k_B/V$ where k_B is the Boltzmann constant and V is the system volume. The normalized thermal conductivity spectrum of the host matrix is presented in Figure 10.

3.3.2 Results and Discussion

The results of the percent decrease in thermal conductivity κ for the rational distribution at various volume fractions f_v are presented in Figure 11. We observe for all f_v tested, like the irrational distributions, the rational distribution possesses a lower thermal conductivity than both the single size distribution with D=1.3 nm and the random alloy. Additionally, the thermal conductivity reduction of the rational distribution is actually less than that of the irrational distributions. As described in the previous sections, this behavior is more likely due to the reduced number of nanoparticles i.e. the particle number density rather than the specific distribution of nanoparticle sizes. Furthermore, we once again observe a decrease in the κ difference between the rational size distribution and the single size distribution as volume fraction f_v increases.

3.4 Nanoparticle-in-Alloy

3.4.1 Introduction

NEMD simulations in this work so far have showed the random alloy composite to be the most performant in thermal conductivity κ reduction from the pure material. A possible explanation for this result, supported by findings in the previous sections, is that particle number density is the most significant factor in affecting lattice thermal transport through a nanoparticle-laden composite. The random alloy can be considered as a single size distribution of maximum particle number density and therefore achieves a maximum in phonon scattering opportunities. However, the alloy impurities are known to strongly scatter short wavelength phonons more so than longer wavelength phonons [3]. Thus, the lattice thermal conductivity is dominated by contributions of the low frequency phonons near the Brillouin Zone center possessing long wavelengths. It has been experimentally shown that the thermal conductivity of a semiconductor alloy can be reduced by embedding dopant nanoparticles which strongly scatter the mid to long wavelength phonons [34]. The study and similar computational investigations, however, only examined the case where the nanoparticle matrix was different than the constituent materials of the alloy [7] [6]. It is still unclear how inclusion of both nanoparticles and alloy impurities of the same matrix affects the thermal conductivity κ of a pure crystalline solid. In this section, we examine the κ values of such "Nanoparticle-in-Alloy" structure.

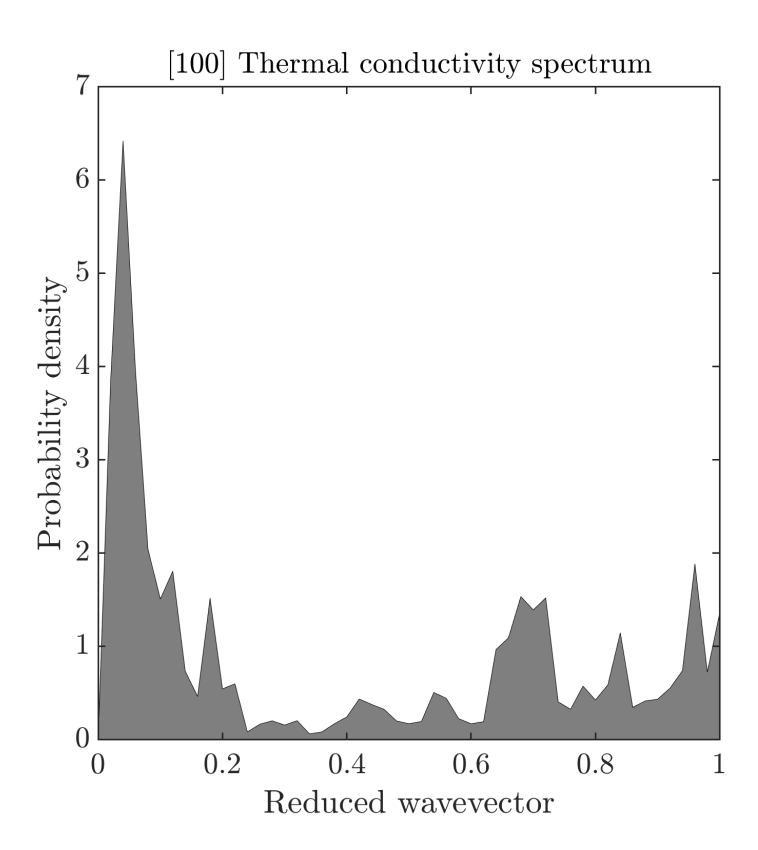


Figure 10: Normalized [100] thermal conductivity spectrum of the host matrix predicted from phonon normal mode analysis in equilibrium molecular dynamics simulations. The nanoparticle size distribution is constructed by equating the normalized thermal conductivity spectrum to a probability density function and equating the phonon wavelengths to the nanoparticle radii.

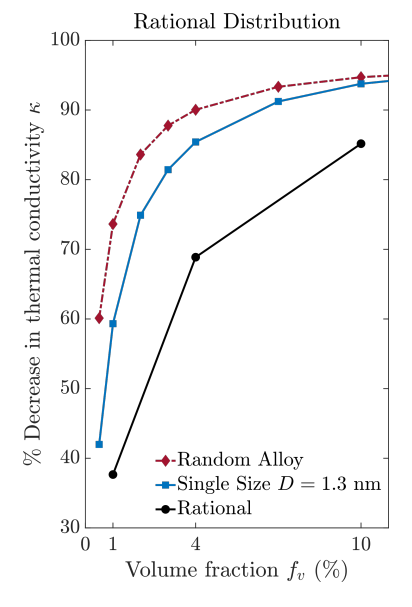


Figure 11: Rational distribution percent decrease in thermal conductivity κ for various volume fractions f_v . For all f_v tested, the rational distribution possesses a lower thermal conductivity than both the single size distribution with D=1.3 nm and the random alloy. Similar to the findings for the irrational distributions, this result is most likely due to the reduced particle number density rather than the specific nanoparticle sizes.

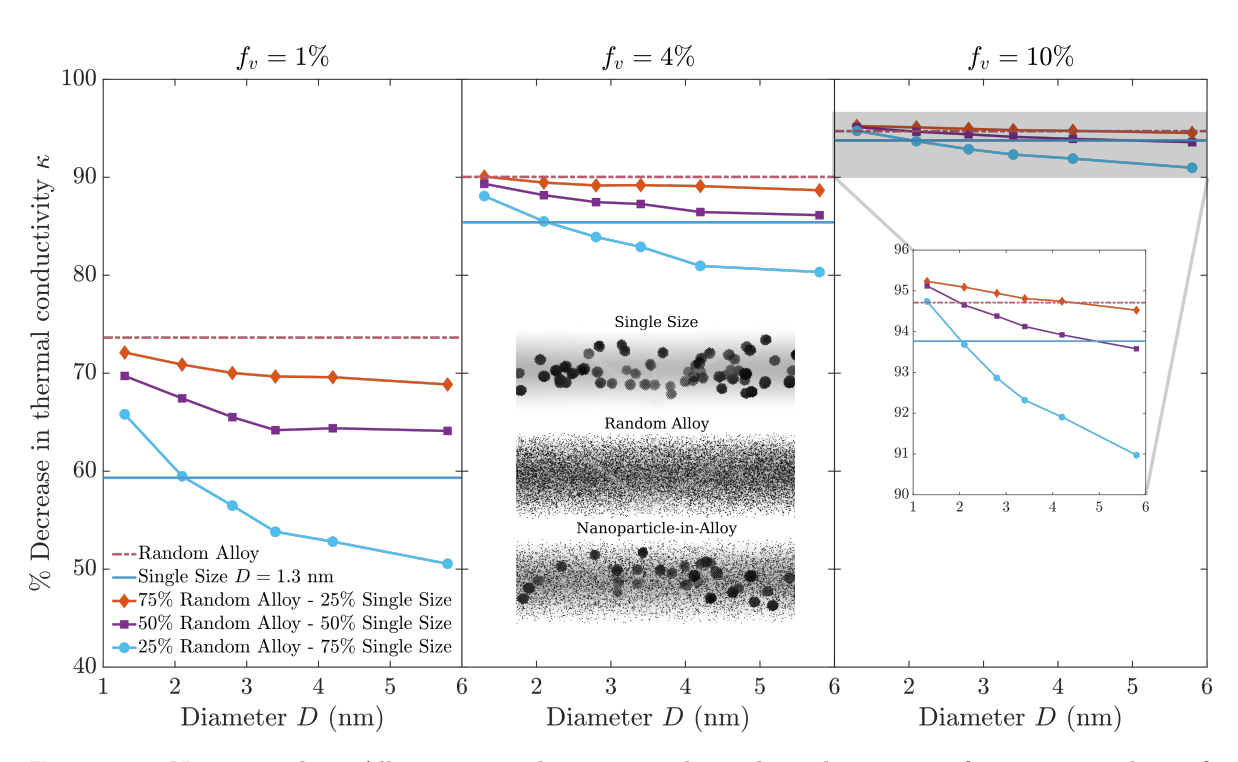


Figure 12: Nanoparticle-in-Alloy percent decrease in thermal conductivity κ for varying values of nanoparticle diameter D at different volume fractions f_v . Like the single size distribution, κ expectedly decreases with decreasing D and increasing random alloy fraction due to the increase in particle number density. This result once again, confirms particle number density as the dominant factor on thermal conductivity at low f_v . At $f_v > 10\%$, we found the configuration with 75% random alloy possessed thermal conductivity lower than the random alloy up to high D. Single size, random alloy, and nanoparticle-in-alloy structures visualized using OVITO [25].

3.4.2 Results and Discussion

For a thorough dissection of the lattice thermal transport through the nanoparticle-in-alloy structure, we study cases where the fractions of nanoparticle volume and random alloy volume are varied while fixing the total dopant volume fraction f_v . We present the percent decrease in thermal conductivity κ for composites containing a single size distribution mixed with the random alloy in Figure 12. Just like the case for the pure single size distribution, nanoparticle-in-alloy structures containing nanoparticles with smaller diameters D possess a larger number of nanoparticles N. The κ reduction of such structures is expectedly larger than configurations with smaller N. Similarly, κ decreases as the fraction of random alloy increases. These results are consistent with previous experimental data of the nanoparticle-in-alloy system [34] [35]. We also observe these structures to be more performant in κ reduction than the single size distribution with D=1.3 nm for all volume fractions f_v tested up to high values of D, however, the nanoparticle-in-alloy does not achieve a thermal conductivity lower than random alloy at low f_v . This result again confirms the dominance of particle number density on thermal conductivity reduction at low volume fractions. At large $f_v > 10\%$, we found the configuration with 75% random alloy possessed thermal conductivity lower than the random alloy up to high D. Though such case is evidence of a nanoparticle size configuration that surpasses the pure random allow in thermal conductivity reduction, the maximum percent decrease from the thermal conductivity of the random alloy is less than 10%. The tested nanoparticle-in-alloy configurations supports our conclusions from the previous sections that at large volume fractions f_v , variation in particle number density or nanoparticle sizes minimally affects the thermal conductivity in comparison to the dopant volume.

4 Conclusions

In summary, we applied NEMD simulations to predict the effective lattice thermal conductivity κ of nanoparticle-laden composites possessing a systematic variety of nanoparticle size distributions. We found that the specific nanoparticle sizes have a minimal influence on κ , with particle number density and volume fraction being the more significant factors. At low volume fractions $f_v < 10\%$, κ decreases considerably with increasing particle number density. Surprisingly, composites possessing a spectrum of nanoparticle sizes were never able to outperform a single size distribution with equivalent particle number density. A possible explanation is that the scattering efficiency of larger sizes is not sufficiently larger than the efficiency of smaller nanoparticles, yet the larger sizes have a more considerable contribution to the dopant volume cost. Essentially, many smaller nanoparticles is likely more "cost-effective" for increased phonon scattering than fewer larger nanoparticles. Additionally, we observed at large volume fractions $f_v > 10\%$, there were minimal differences in κ for differences in particle number density and nanoparticle sizes. This result is likely attributed to the reduction in clearance between nanoparticles far below the mean free paths of phonons in the pure material. At this point, there is significant multiple phonon scattering and so an average scatterer composition manifests. More precisely, different phonons are scattered by approximately the same sample of nanoparticle sizes so variation in sizes and scatterer density is negligible. The random alloy configuration achieved the lowest κ for all $f_v < 10\%$ and was only surpassed by a nanoparticle-in-alloy distribution at $f_v > 10\%$, but only by a less than 10% decrease from the random alloy thermal conductivity. It is possible there exists some nanoparticle size distribution more performant in κ reduction than the configurations explored in this work, however, determining and fabricating such distribution may not be worth the effort. Instead, we recommend material engineers to focus more on making the nanoparticles as small as possible and develop strategies to minimize particle aggregation and grain growth during manufacturing of thermoelectric materials. Such processes would maximize phonon scattering and result in a lattice thermal conductivity minimum.

5 Credit Author Statement

Theodore Maranets: Conceptualization, Formal analysis, Software, Writing - Original Draft, Writing - Review and Editing. Haoran Cui: Software, Writing - Original Draft, Writing - Review and Editing. Yan Wang: Conceptualization, Formal analysis, Supervision, Writing - Original Draft, Writing - Review and Editing.

6 Declaration of Competing Interest

The authors declare that they have no known competing financial interests or personal relationships that could have appeared to influence the work reported in this paper.

7 Data Availability

Data will be made available on reasonable request.

8 Acknowledgements

The authors thank the support from the Nuclear Regulatory Commission (award number: 31310021M0004) and the National Science Foundation (award number: 2047109). The authors also would like to acknowledge the support of Research & Innovation and the Cyberinfrastructure Team in the Office of Information Technology at the University of Nevada, Reno for facilitation and access to the Pronghorn High-Performance Computing Cluster.

References

- [1] Mildred S Dresselhaus, Gang Chen, Ming Y Tang, RG Yang, Hohyun Lee, DZ Wang, ZF Ren, J-P Fleurial, and Pawan Gogna. New directions for low-dimensional thermoelectric materials. *Advanced materials*, 19(8):1043–1053, 2007.
- [2] Adrian Bejan and Allan D Kraus. Heat transfer handbook, volume 1. John Wiley & Sons, 2003.
- [3] John M Ziman. Electrons and phonons: the theory of transport phenomena in solids. Oxford university press, 2001.
- [4] Takuma Hori and Junichiro Shiomi. Tuning phonon transport spectrum for better thermoelectric materials. Science and technology of advanced materials, 20(1):10–25, 2019.
- [5] Yi Ma, Richard Heijl, and Anders EC Palmqvist. Composite thermoelectric materials with embedded nanoparticles. *Journal of Materials Science*, 48:2767–2778, 2013.
- [6] N Mingo, D Hauser, NP Kobayashi, M Plissonnier, and A Shakouri. "nanoparticle-in-alloy" approach to efficient thermoelectrics: silicides in sige. *Nano letters*, 9(2):711–715, 2009.
- [7] Joseph P Feser. Engineering heat transport in nanoparticle-in-alloy composites: The role of mie scattering. *Journal of Applied Physics*, 125(14), 2019.
- [8] Hang Zhang and Austin J Minnich. The best nanoparticle size distribution for minimum thermal conductivity. *Scientific reports*, 5(1):8995, 2015.
- [9] Woochul Kim and Arun Majumdar. Phonon scattering cross section of polydispersed spherical nanoparticles. *Journal of Applied Physics*, 99(8), 2006.
- [10] Neil Zuckerman and Jennifer R Lukes. Acoustic phonon scattering from particles embedded in an anisotropic medium: A molecular dynamics study. *Physical Review B*, 77(9):094302, 2008.
- [11] Anupam Kundu, Natalio Mingo, DA Broido, and DA Stewart. Role of light and heavy embedded nanoparticles on the thermal conductivity of sige alloys. *Physical Review B*, 84(12):125426, 2011.
- [12] Rohit R Kakodkar and Joseph P Feser. Wavevector and polarization resolved analysis of phonon scattering from embedded nanoparticles. *Journal of Applied Physics*, 124(8), 2018.
- [13] Theodore Maranets and Yan Wang. Ballistic phonon lensing by the non-planar interfaces of embedded nanoparticles [in press]. New Journal of Physics, 2023.
- [14] Alan JH McGaughey and M Kaviany. Phonon transport in molecular dynamics simulations: formulation and thermal conductivity prediction. *Advances in heat transfer*, 39:169–255, 2006.

- [15] John Edward Jones. On the determination of molecular fields.—ii. from the equation of state of a gas. Proceedings of the Royal Society of London. Series A, Containing Papers of a Mathematical and Physical Character, 106(738):463–477, 1924.
- [16] Weishu Liu, Xiao Yan, Gang Chen, and Zhifeng Ren. Recent advances in thermoelectric nanocomposites. *Nano Energy*, 1(1):42–56, 2012.
- [17] Maria N Luckyanova, Jivtesh Garg, Keivan Esfarjani, Adam Jandl, Mayank T Bulsara, Aaron J Schmidt, Austin J Minnich, Shuo Chen, Mildred S Dresselhaus, Zhifeng Ren, et al. Coherent phonon heat conduction in superlattices. *Science*, 338(6109):936–939, 2012.
- [18] Pranay Chakraborty, Isaac Armstrong Chiu, Tengfei Ma, and Yan Wang. Complex temperature dependence of coherent and incoherent lattice thermal transport in superlattices. *Nanotechnology*, 32(6):065401, 2020.
- [19] Pranay Chakraborty, Yida Liu, Tengfei Ma, Xixi Guo, Lei Cao, Run Hu, and Yan Wang. Quenching thermal transport in aperiodic superlattices: A molecular dynamics and machine learning study. ACS applied materials & interfaces, 12(7):8795–8804, 2020.
- [20] Samuel C Huberman, Jason M Larkin, Alan JH McGaughey, and Cristina H Amon. Disruption of superlattice phonons by interfacial mixing. *Physical Review B*, 88(15):155311, 2013.
- [21] ES Landry, MI Hussein, and AJH McGaughey. Complex superlattice unit cell designs for reduced thermal conductivity. *Physical Review B*, 77(18):184302, 2008.
- [22] Yan Wang, Haoxiang Huang, and Xiulin Ruan. Decomposition of coherent and incoherent phonon conduction in superlattices and random multilayers. *Physical Review B*, 90(16):165406, 2014.
- [23] Yan Wang, Chongjie Gu, and Xiulin Ruan. Optimization of the random multilayer structure to break the random-alloy limit of thermal conductivity. *Applied Physics Letters*, 106(7), 2015.
- [24] B Abeles. Lattice thermal conductivity of disordered semiconductor alloys at high temperatures. *Physical Review*, 131(5):1906, 1963.
- [25] Alexander Stukowski. Visualization and analysis of atomistic simulation data with ovito—the open visualization tool. *Modelling and simulation in materials science and engineering*, 18(1):015012, 2009
- [26] Patrick K Schelling, Simon R Phillpot, and Pawel Keblinski. Comparison of atomic-level simulation methods for computing thermal conductivity. *Physical Review B*, 65(14):144306, 2002.
- [27] Daniel P Sellan, Eric S Landry, JE Turney, Alan JH McGaughey, and Cristina H Amon. Size effects in molecular dynamics thermal conductivity predictions. *Physical Review B*, 81(21):214305, 2010.
- [28] Aidan P Thompson, H Metin Aktulga, Richard Berger, Dan S Bolintineanu, W Michael Brown, Paul S Crozier, Pieter J in't Veld, Axel Kohlmeyer, Stan G Moore, Trung Dac Nguyen, et al. Lammps-a flexible simulation tool for particle-based materials modeling at the atomic, meso, and continuum scales. Computer Physics Communications, 271:108171, 2022.
- [29] Bowen Cai, Jun Pei, Jinfeng Dong, Hua-Lu Zhuang, Jinyu Gu, Qian Cao, Haihua Hu, Zihao Lin, and Jing-Feng Li. (bi, sb) 2te3/sic nanocomposites with enhanced thermoelectric performance: Effect of sic nanoparticle size and compositional modulation. *Science China Materials*, 64(10):2551–2562, 2021.
- [30] John Androulakis, Iliya Todorov, Jiaqing He, Duck-Young Chung, Vinayak Dravid, and Mercouri Kanatzidis. Thermoelectrics from abundant chemical elements: high-performance nanostructured pbse–pbs. *Journal of the American Chemical Society*, 133(28):10920–10927, 2011.
- [31] Lipeng Hu, Fanchen Meng, Yanjie Zhou, Jibiao Li, Allen Benton, Junqin Li, Fusheng Liu, Chaohua Zhang, Heping Xie, and Jian He. Leveraging deep levels in narrow bandgap bi0. 5sb1. 5te3 for record-high ztave near room temperature. Advanced Functional Materials, 30(45):2005202, 2020.

- [32] Sanyukta Ghosh, Sahil Tippireddy, Gyan Shankar, Anirudha Karati, Gerda Rogl, Peter Rogl, Ernst Bauer, Sai Rama Krishna Malladi, BS Murty, Satyam Suwas, et al. Insb nanoparticles dispersion in yb-filled co4sb12 improves the thermoelectric performance. *Journal of Alloys and Compounds*, 880:160532, 2021.
- [33] Tianli Feng, Xiulin Ruan, Zhenqiang Ye, and Bingyang Cao. Spectral phonon mean free path and thermal conductivity accumulation in defected graphene: The effects of defect type and concentration. *Physical Review B*, 91(22):224301, 2015.
- [34] Woochul Kim, Joshua Zide, Arthur Gossard, Dmitri Klenov, Susanne Stemmer, Ali Shakouri, and Arun Majumdar. Thermal conductivity reduction and thermoelectric figure of merit increase by embedding nanoparticles in crystalline semiconductors. *Physical review letters*, 96(4):045901, 2006.
- [35] Jing-Feng Li, Wei-Shu Liu, Li-Dong Zhao, and Min Zhou. High-performance nanostructured thermoelectric materials. *NPG Asia Materials*, 2(4):152–158, 2010.